J. Fluid Mech. (1986), vol. 162, pp. 23–33
Printed in Great Britain


# The effect of rotation on double-diffusive interleaving

By OLIVER S. KERR AND JUDITH Y. HOLYER
School of Mathematics, Bristol University, Bristol, England BS8 1TW

(Received 22 January 1985 and in revised form 11 July 1985)

In this paper we investigate the effect of vertical rotation on the linear stability of an unbounded region of vertically stratified fluid, which has compensating horizontal temperature and salinity gradients, so there is no overall horizontal density gradient. We find the most unstable perturbations for given linear vertical and horizontal gradients and show how the addition of rotation affects the results found for the non-rotating case by Holyer (1983), using molecular diffusivities. By using a transformation that, for the non-oscillatory instability, links the rotating case to the non-rotating case we show that the growth rate, the across-front slope and the wavenumber of the intrusion with the maximum growth rate is unchanged. The basic difference between the non-rotating and the rotating case, for the non-oscillatory instability, is that in the rotating case the interleaving layers slope both along and perpendicular to the direction of the horizontal temperature and salinity gradients and not just along them. The oscillatory instability has no simple transformation between the rotating and the non-rotating cases, and the addition of rotation changes the growth rate and the wavenumber of the instabilities.

## 1. Introduction

A stratified fluid with horizontal temperature and salinity gradients, but no horizontal density gradient is unstable to infinitesimal perturbations (Holyer 1983). This statement is true even when the salinity increases with depth and the temperature decreases with depth, so that both components that contribute to the vertical density gradient are stably stratified. This situation has been studied in the laboratory by Thorpe, Hutt & Soulsby (1969), Wirtz, Briggs & Chen (1972) and Ruddick & Turner (1979), who all observed the formation of interleaving layers. Similar layers have been observed in the ocean by Stommel & Fedorov (1967), Horne (1978) and Gregg (1980).

These intrusions have been investigated theoretically by Stern (1967), Toole & Georgi (1981) and Posmentier & Hibbard (1982) using the assumption that salt fingers are already present. They assume that the heat and salt fluxes are purely vertical, driven by the salt fingering. They model these fluxes by using uniform eddy diffusivities and taking the ratio of the heat flux to the salt flux to be a constant $\gamma$. McDougall (1985) has also used vertical fluxes, but assumes that the fluxes are proportional to the salinity difference between the intrusions but are independent of their thickness. The models used by these authors all require the presence of salt fingers for the interleaving to occur, which is usually the case if the background salt gradient is unstable. Toole & Georgi (1981) argue that in the oceans the assumption that the fluxes are dominated by the salt-finger fluxes could also be valid for a stable background salt gradient. The laboratory experiments show that interleaving occurs even when the salt gradient is stable and there are initially no salt fingers, a situation in which earlier models are not applicable. Holyer (1983) shows, using molecular diffusivities for heat, salt and momentum, how the interleaving instability develops and how the linear instability can grow until salt fingers appear.

In this paper we extend the work of Holyer to include the effect of vertical rotation, which will be important to large-scale oceanographic applications and which may also be relevant to stellar dynamics (Knobloch & Spruit 1983). Holyer looked at the case with no rotation and determined the fastest-growing modes for given temperature and salinity gradients. Worthem, Mollo-Christensen & Ostapoff (1983) considered the effects of rotation, shear and horizontal gradients on the stability of an unbounded stratified fluid. They derived a characteristic equation similar to that obtained by Baines & Gill (1969) in their investigation of double-diffusive convection due to linear vertical gradients between horizontal stress-free boundaries. They then used this to investigate the stability boundaries of disturbances with no along-front structure.

We show that with horizontal gradients and rotation the model is always unstable to some disturbance, and so there are no stability boundaries. We allow along-front structure and determine maximum growth-rate disturbances.

In §2 we obtain the linear stability equations. In §3 the non-oscillatory instability, where the growth rate is real, is considered. In §4 we look at the oscillatory instability and how it alters as the rotation changes.

## 2. The linear stability problem

We consider an unbounded region of incompressible, rotating, stratified fluid. We assume that there is no horizontal density gradient, so that any horizontal temperature gradient present is balanced by a horizontal salinity gradient. The vertical temperature and salinity gradients may be either stabilizing or destabilizing. The rotation is assumed to be about a vertical axis. We look at the case where the undisturbed state has linear gradients of temperature and salinity, in both the horizontal and the vertical directions. The coordinates are chosen so that the $z$-axis is vertically upwards and the $x$-axis is parallel to the horizontal gradients. The $y$-axis will then lie in the horizontal, perpendicular to the horizontal gradients. With these coordinates the undisturbed temperature and salinity fields are given by

$$T_0+\bar{T}_x x+\bar{T}_z z, \quad S_0+\bar{S}_x x+\bar{S}_z z, \tag{2.1}$$

where $\bar{T}_x$, $\bar{T}_z$, $\bar{S}_x$ and $\bar{S}_z$ are constants. We assume that the density $\rho$ depends linearly on the temperature and salinity, so

$$\rho = \rho_0(1-\alpha(T-T_0)+\beta(S-S_0)), \tag{2.2}$$

where $T$ and $S$ are the temperature and salinity and $\alpha$ and $\beta$ are positive constants. Since we require that there is no horizontal density gradient

$$\alpha\bar{T}_x = \beta\bar{S}_x. \tag{2.3}$$

We choose the $x$-direction so that $\bar{S}_x$ is positive, which means that at any given depth the amount of salt increases as $x$ increases.

Making the Boussinesq approximation and letting the rotation rate for the system be $\frac{1}{2}\boldsymbol{f}$, with $\boldsymbol{f}=f\hat{\boldsymbol{z}}$, the equations for the infinitesimal perturbations, $\boldsymbol{u}$, $T$, $S$ and $p$ to the velocity, temperature, salinity and modified pressure are

$$\frac{\partial \boldsymbol{u}}{\partial t}+\boldsymbol{f}\wedge\boldsymbol{u} = -\frac{1}{\rho_0}\nabla p+g(\alpha T-\beta S)\hat{\boldsymbol{z}}+\nu\nabla^2\boldsymbol{u}, \tag{2.4a}$$

$$\frac{\partial T}{\partial t}+u\bar{T}_x+w\bar{T}_z = \kappa_T \nabla^2 T, \tag{2.4b}$$

$$\frac{\partial S}{\partial t}+u\bar{S}_x+w\bar{S}_z = \kappa_S \nabla^2 S, \tag{2.4c}$$

$$\nabla \cdot \boldsymbol{u} = 0, \tag{2.4d}$$

where $\boldsymbol{u} = (u, v, w).$

These equations are manipulated to give an equation for $u$:

$$\left(\frac{\partial}{\partial t}-\nu\nabla^2\right)\left\{\left(\frac{\partial}{\partial t}-\nu\nabla^2\right)\left(\frac{\partial}{\partial t}-\kappa_T\nabla^2\right)\left(\frac{\partial}{\partial t}-\kappa_S\nabla^2\right)\nabla^2+g\alpha\bar{T}_z\left(\frac{\partial}{\partial t}-\kappa_S\nabla^2\right)\left(\frac{\partial^2}{\partial x^2}+\frac{\partial^2}{\partial y^2}\right)\right.$$
$$\left.-g\beta\bar{S}_z\left(\frac{\partial}{\partial t}-\kappa_T\nabla^2\right)\left(\frac{\partial^2}{\partial x^2}+\frac{\partial^2}{\partial y^2}\right)-g\beta\bar{S}_x(\kappa_T-\kappa_S)\nabla^2\frac{\partial^2}{\partial x\,\partial z}\right\}u$$
$$+f^2\left(\frac{\partial}{\partial t}-\kappa_T\nabla^2\right)\left(\frac{\partial}{\partial t}-\kappa_S\nabla^2\right)\frac{\partial^2}{\partial z^2}u-fg\beta\bar{S}_x(\kappa_T-\kappa_S)\nabla^2\frac{\partial^2}{\partial y\,\partial z}u = 0. \tag{2.5}$$

This is a linear equation with constant coefficients and so we can express the solution as the superposition of solutions of the form

$$u = \mathrm{Re}\{u_0 \exp(\mathrm{i}\boldsymbol{k}\cdot\boldsymbol{x}+\lambda t)\}, \tag{2.6}$$

where $u_0$ is a complex constant, $\boldsymbol{k} = (k, l, m)$ is the wavenumber vector and $\lambda$ is the growth rate, which can be complex. Substituting this solution into (2.5) gives us the characteristic equation

$$(\lambda+\nu\mu^2)\left\{(\lambda+\nu\mu^2)(\lambda+\kappa_T\mu^2)(\lambda+\kappa_S\mu^2)\mu^2+\lambda g(\alpha\bar{T}_z-\beta\bar{S}_z)(k^2+l^2)\right.$$
$$\left.+(k^2+l^2)\mu^2 g\kappa_T\kappa_S\left(\frac{\alpha\bar{T}_z}{\kappa_T}-\frac{\beta\bar{S}_z}{\kappa_S}\right)+g\beta\bar{S}_x(\kappa_T-\kappa_S)\mu^2 km\right\}$$
$$+f^2m^2(\lambda+\kappa_T\mu^2)(\lambda+\kappa_S\mu^2)+fg\beta\bar{S}_x(\kappa_T-\kappa_S)\mu^2 lm = 0, \tag{2.7}$$

where $\mu = (k^2+l^2+m^2)^{\frac{1}{2}}$ is the wavenumber. This solution is unstable if $\mathrm{Re}\{\lambda\} > 0$ and is neutrally stable if $\mathrm{Re}\{\lambda\} = 0$, when either $\lambda = 0$ or $\lambda$ is pure imaginary. When $\lambda = 0$, this is the case of marginal stability for a non-oscillatory exponentially growing disturbance, and, when $\lambda$ is pure imaginary, this is the case of marginal stability for an oscillatory exponentially growing disturbance. We look at the cases of steady and oscillatory growth of instabilities separately in §§3 and 4 respectively.

## 3. Steady growth

When the solution is neutrally stable to a non-oscillatory instability $\lambda = 0$. Substituting into (2.7) gives

$$\nu^2\kappa_T\kappa_S\mu^{10}+f^2\kappa_T\kappa_S m^2\mu^4 = -\nu\mu^4 g\kappa_T\kappa_S\left(\frac{\alpha\bar{T}_z}{\kappa_T}-\frac{\beta\bar{S}_z}{\kappa_S}\right)(k^2+l^2)$$
$$-\nu\mu^4 kmg\beta\bar{S}_x(\kappa_T-\kappa_S)$$
$$-fg\beta\bar{S}_x(\kappa_T-\kappa_S)ml\mu^2. \tag{3.1}$$

Considering the left- and right-hand sides separately, the left-hand side of (3.1) is always positive, and for fixed ratios of $k$, $l$ and $m$ is $O(\mu^{10})$ as $\mu \rightarrow \infty$, while the right-hand side is $O(\mu^6)$. So for sufficiently large $\mu$ the left-hand side of (3.1) will be greater than the right-hand side. Similarly, as $\mu \rightarrow 0$ the left-side is $O(\mu^6)$ while the right side is dominated by the last term, which is $O(\mu^4)$ provided $\bar{S}_x \neq 0$. If this last term is positive then the left-hand side becomes smaller than the right-hand side as $\mu \rightarrow 0$, and so there is some $\mu$ such that both sides are equal and hence there is a solution. So we see that there is a point of neutral stability for any given salt and temperature gradients, provided $\bar{S}_x \neq 0$. Since there is a mode of marginal stability, which is on the border between stability and instability, we must also have for any given set of gradients a mode which is unstable provided the last term on the right-hand side of (3.1) is positive. Since $\kappa_T > \kappa_S$ and $\bar{S}_x > 0$ this gives

$$flm < 0. \tag{3.2}$$

Since we are not restricted in the choice of the sign of $l$ and $m$ we can always find a mode that satisfies this condition and is unstable. This condition implies that if there is a horizontal gradient of temperature and salinity then the fluid is always unstable to a non-oscillatory disturbance, just as in the non-rotating case.

We now look for the instabilities with the largest growth rate. For non-oscillatory growth this occurs when

$$\frac{\partial \lambda}{\partial k} = \frac{\partial \lambda}{\partial l} = \frac{\partial \lambda}{\partial m} = 0. \tag{3.3}$$

We differentiate the characteristic equation (2.7) with respect to the wavenumber-vector components $k$, $l$, and $m$ and get three equations that are to be solved simultaneously with (2.7) to find the values of $\lambda$, $k$, $l$ and $m$ that maximize the growth rate. By adding suitable multiples of these we obtain the following three equations that have to be satisfied along with (2.7):

$$fk = l(\lambda + \nu\mu^2); \tag{3.4}$$

$$0 = k\lambda g(\alpha\bar{T}_z - \beta\bar{S}_z) + k\mu^2 g\kappa_T\kappa_S\left(\frac{\alpha\bar{T}_z}{\kappa_T} - \frac{\beta\bar{S}_z}{\kappa_S}\right) + \mu^2[m^2 - (k^2+l^2)]\frac{g\beta\bar{S}_x}{zm}(\kappa_T - \kappa_S) - fl(\lambda + \kappa_T\mu^2)(\lambda + \kappa_S\mu^2); \tag{3.5}$$

$$\begin{aligned} 0 = {} & (2\nu + \kappa_T + \kappa_S)\lambda^3 + 2(\nu^2 + 2\nu\kappa_T + 2\nu\kappa_S + \kappa_T\kappa_S)\lambda^2\mu^2 \\ & + 3(\nu^2\kappa_T + \nu^2\kappa_S + 2\nu\kappa_T\kappa_S)\lambda\mu^4 + 4\nu^2\kappa_T\kappa_S\mu^6 \\ & + \nu kmg\beta\bar{S}_x(\kappa_T - \kappa_S) + \frac{k}{2m}(\lambda + \nu\mu^2)g\beta\bar{S}_x(\kappa_T - \kappa_S) \\ & - \frac{\lambda^2}{\mu^4}(k^2+l^2)g(\alpha\bar{T}_z - \beta\bar{S}_z) + \nu(k^2+l^2)g\kappa_T\kappa_S\left(\frac{\alpha\bar{T}_z}{\kappa_T} - \frac{\beta\bar{S}_z}{\lambda_S}\right) \\ & + f^2m^2\left(-\frac{\lambda^2}{\mu^4} + \kappa_S\kappa_T\right) + \frac{f^2}{\mu^2}(\lambda + \kappa_T\mu^2)(\lambda + \kappa_S\mu^2) + \frac{fl}{2m}g\beta\bar{S}_x(\kappa_T - \kappa_S). \end{aligned} \tag{3.6}$$

Equation (3.4) is analogous to results obtained by Posmentier & Hibbard (1982) and McDougall (1985) in their models that used eddy diffusivities and eddy-flux

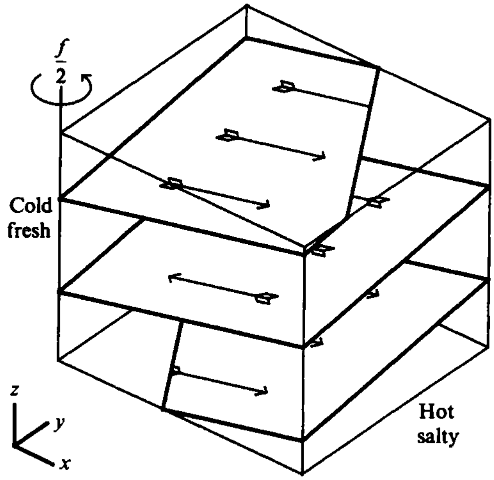


FIGURE 1. Schematic illustration of the slope of the fastest-growing direct mode of instability with $f > 0$.

coefficients respectively. If (3.4) is substituted into the equation for the vertical vorticity we get the result that for the fastest-growing mode

$$v = 0. \tag{3.7}$$

Figure 1 gives a schematic illustration of the intrusions for the non-oscillatory mode, showing how the intrusions slope.

Equations (3.4) and (3.7) give us the results found in the appendix of Holyer, that for the non-rotating case the fastest-growing disturbances are two-dimensional ones that go across the front ($v = 0$, $l = 0$).

In the rotating case if we assume that a disturbance has $v = 0$ then we retrieve (3.4). So if we take $l = 0$, as assumed by Worthem *et al.* (1983), then the disturbances must have an along-front velocity component ($v \neq 0$) and will not then be parallel to the $(x, z)$-plane. More importantly we would be excluding from consideration the fastest-growing modes.

We now non-dimensionalize the equations for maximum growth. We define

$$q = \frac{\lambda}{\kappa_T \mu^2}, \quad F = \frac{f}{\kappa_T \mu^2},$$

$$H = \frac{g\beta \bar{S}_x}{\nu \kappa_T \mu^4}, \quad R_T = \frac{g\alpha \bar{T}_z}{\nu \kappa_T \mu^4}, \quad R_S = \frac{g\beta \bar{S}_z}{\nu \kappa_T \mu^4}, \tag{3.8}$$

where $H$ is the horizontal Rayleigh number and $R_T$ and $R_S$ are the vertical thermal and saline Rayleigh numbers.

We also define

$$\sigma = \frac{\nu}{\kappa_T}, \quad \tau = \frac{\kappa_S}{\kappa_T}, \tag{3.9}$$

where $\sigma$ is the Prandtl number and $\tau$ the salt-to-heat diffusivity ratio.

By manipulating (2.7), (3.4), (3.5) and (3.6) we get the following non-dimensional equations:

$$F = \frac{l}{k}(q+\sigma); \tag{3.10a}$$

$$H = -\frac{2m}{k}\frac{1}{\sigma(1-\tau)}(q+\sigma)(q+1)(q+\tau); \tag{3.10b}$$

$$R_T = \frac{k^2+m^2}{k^2}\frac{q+1}{\sigma q(1-\tau)}\left[-q^3+q(\sigma\tau+\sigma+\tau)+2\sigma\tau+\frac{k^2-m^2}{k^2+m^2}q(q+\sigma)(q+\tau)\right]; \quad (3.10c)$$

$$R_S = \frac{k^2+m^2}{k^2}\frac{q+\tau}{\sigma q(1-\tau)}\left[-q^3+q(\sigma\tau+\sigma+\tau)+2\sigma\tau+\frac{k^2-m^2}{k^2+m^2}q(q+\sigma)(q+1)\right]. \quad (3.10d)$$

These last three are identical to the equations for the non-rotating case found by Holyer (in her case $\mu^2 = k^2+m^2$). These are only dependent on the ratio $k/m$, $q$ and, via the non-dimensionalization, $\mu$. Thus for any given gradients $\bar{S}_x$, $\bar{T}_z$, $\bar{S}_z$, if we find a solution with the same $\lambda$, $k/m$ and $\mu$ as for the non-rotating case, then the last three equations will be automatically satisfied. Then we only have to satisfy (3.10$a$). Suppose that, for the given gradients, the non-rotating case has a fastest-growing mode with

$$\lambda = \lambda_0, \quad \boldsymbol{k} = (k_0, 0, m_0). \quad (3.11)$$

Then, if we add rotation we find that

$$\lambda = \lambda_0, \quad \boldsymbol{k} = (k_0 \cos\theta, (k_0^2+m_0^2)^{\frac{1}{2}} \sin\theta, m_0 \cos\theta), \quad (3.12a)$$

where

$$\tan\theta = \frac{fk_0}{(\lambda_0+\nu\mu_0^2)(k_0^2+m_0^2)^{\frac{1}{2}}} \quad (3.12b)$$

satisfies the conditions of not altering $\lambda$, $k/m$ and $\mu$, and also satisfies (3.10$a$) and so is the fastest-growing mode for the rotating case.

This tells us that the fastest-growing mode has the same growth rate, across-front slope, $m_0/k_0$, and absolute wavenumber as the system would have if it was non-rotating with the same temperature and salinity gradients. The only effect of the rotation is to tilt the fastest-growing intrusions along the front, while leaving the growth rate unchanged. As the rotation rate increases the wave vector $\boldsymbol{k}$ tends towards being parallel with the front. Similar behaviour is also found by McDougall (1985). The wave vector is expected to become horizontal, since, in the limit of $f\rightarrow\infty$, we would expect the fluid to obey Proudman's theorem and be independent of $z$. The transition occurs when the rotation rate is of order $\nu\mu_0^2$.

If, instead of using molecular diffusivities, we use eddy diffusivities appropriate to the ocean, then the effects of the Earth's rotation would be to tilt the intrusions along the front. This along-front slope would in general be less than the across-front slope and the vertical wavenumber $m$ would be virtually unaffected by the rotation. The more extreme behaviour with the wavenumber vector aligning itself with the front would be outside the parameter ranges found in the oceans.

## 4. Oscillatory growth

When the system is neutrally stable to an oscillatory mode, $\lambda$ is purely imaginary. If we set $\lambda = \mathrm{i}\omega$, with $\omega$ real, into the characteristic equation (2.7) and take real and imaginary parts we get the following pair of equations:

$$\nu\mu^2\left[\nu\kappa_T\kappa_S\mu^8+km\mu^2g\beta\bar{S}_x(\kappa_T-\kappa_S)+(k^2+l^2)\mu^2g\kappa_T\kappa_S\left(\frac{\alpha\bar{T}_z}{\kappa_T}-\frac{\beta\bar{S}_z}{\kappa_S}\right)\right]$$
$$+f^2m^2\kappa_T\kappa_S\mu^4+flmg\beta\bar{S}_x(\kappa_T-\kappa_S)\mu^2-\omega^2\Big[(\nu^2+2\nu\kappa_T+2\nu\kappa_S+\kappa_T\kappa_S)\mu^6$$
$$+(k^2+l^2)g(\alpha\bar{T}_z-\beta\bar{S}_z)+f^2m^2\Big]+\omega^4\mu^2 = 0; \quad (4.1a)$$

$$(\nu^2\kappa_T+\nu^2\kappa_S+2\nu\kappa_T\kappa_S)\mu^6+kmg\beta\bar{S}_x(\kappa_T-\kappa_S)$$
$$+\nu(k^2+l^2)g(\alpha\bar{T}_z-\beta\bar{S}_z)+(k^2+l^2)g\kappa_T\kappa_S\left(\frac{\alpha\bar{T}_z}{\kappa_T}-\frac{\beta\bar{S}_z}{\kappa_S}\right)$$
$$+f^2m^2(\kappa_T+\kappa_S)-(2\nu+\kappa_T+\kappa_S)\mu^2\omega^2=0. \quad (4.1b)$$

In order that a solution to these equations exists with real components of $\boldsymbol{k}$, we find that, when the vertical density gradient is stable ($\alpha\bar{T}_z>\beta\bar{S}_z$) and salt fingering is not possible in the basic state ($(\alpha\bar{T}_z/\kappa_T)-(\beta\bar{S}_z/\kappa_S)>0$), then the following inequality has to be satisfied:

$$\beta\bar{S}_x(\kappa_T-\kappa_S)\frac{km}{k^2+l^2}$$
$$\times\left[1+\frac{fl(2\nu+\kappa_T+\kappa_S)^2\mu^2}{k\left[2\nu(\nu+\kappa_T)(\nu+\kappa_S)\mu^4+\frac{km}{\mu^2}g\beta\bar{S}_x(\kappa_T-\kappa_S)+g\frac{k^2+l^2}{\mu^2}[(\nu+\kappa_S)\alpha\bar{T}_z-(\nu+\kappa_T)\beta\bar{S}_z]\right]}\right]$$
$$>\alpha\bar{T}_z(\nu+\kappa_T)-\beta\bar{S}_z(\nu+\kappa_S). \quad (4.2)$$

When $f=0$ this gives the same condition as Holyer for a stably stratified fluid. The values of $km/(k^2+l^2)$ and $fl/k$ can always be chosen so that (4.2) is satisfied. This condition is a necessary condition for instability, but not a sufficient one.

As with the non-oscillatory instabilities, we look for the mode with the fastest growth rate. This is the mode that has the largest value of $\mathrm{Re}\{\lambda\}$. Substituting $\lambda=\lambda_r+\mathrm{i}\omega$ into (2.7), with $\lambda_r$ and $\omega$ real and $\omega\neq 0$, we obtain, after taking real and imaginary parts, the following pair of equations:

$$(\lambda_r+\nu\mu^2)\Big[(\lambda_r+\nu\mu^2)(\lambda_r+\kappa_T\mu^2)(\lambda_r+\kappa_S\mu^2)\mu^2+km\mu^2g\beta\bar{S}_x(\kappa_T-\kappa_S)$$
$$+\lambda_r(k^2+l^2)g(\alpha\bar{T}_z-\beta\bar{S}_z)+(k^2+l^2)\mu^2g\kappa_T\kappa_S\left(\frac{\alpha\bar{T}_z}{\kappa_T}-\frac{\beta\bar{S}_z}{\kappa_S}\right)\Big]$$
$$+f^2m^2(\lambda_r+\kappa_T\mu^2)(\lambda_r+\kappa_S\mu^2)+flmg\beta\bar{S}_x(\kappa_T-\kappa_S)\mu^2$$
$$-\omega^2[6\lambda_r^2\mu^2+3\lambda_r(2\nu+\kappa_T+\kappa_S)\mu^4+(\nu^2+2\nu\kappa_T+2\nu\kappa_S+\kappa_T\kappa_S)\mu^6$$
$$+(k^2+l^2)g(\alpha\bar{T}_z-\beta\bar{S}_z)+f^2m^2]+\omega^4\mu^2=0; \quad (4.3a)$$

$$4\lambda_r^3\mu^2+3(2\nu+\kappa_T\kappa_S)\lambda_r^2\mu^4+2(\nu^2+2\nu\kappa_T+2\nu\kappa_S+\kappa_T\kappa_S)\lambda_r\mu^6$$
$$+(\nu^2\kappa_T+\nu^2\kappa_S+2\nu\kappa_T\kappa_S)\mu^8+km\mu^2g\beta\bar{S}_x(\kappa_T-\kappa_S)+(2\lambda_r+\nu\mu^2)(k^2+l^2)g(\alpha\bar{T}_z-\beta\bar{S}_z)$$
$$+(k^2+l^2)\mu^2g\kappa_T\kappa_S\left(\frac{\alpha\bar{T}_z}{\kappa_T}-\frac{\beta\bar{S}_z}{\kappa_S}\right)+f^2m^2(2\lambda_r+(\kappa_T+\kappa_S)\mu^2)$$
$$-(4\lambda_r+(2\nu+\kappa_T+\kappa_S)\mu^2)\mu^2\omega^2=0. \quad (4.3b)$$

For the fastest-growing mode we have

$$\frac{\partial\lambda_r}{\partial k}=\frac{\partial\lambda_r}{\partial l}=\frac{\partial\lambda_r}{\partial m}=0. \quad (4.4)$$

Differentiating (4.3*a*) and (4.3*b*) with respect to $k$, $l$ and $m$ gives us three pairs of equations that have to be solved simultaneously with (4.3*a*) and (4.3*b*) to yield the mode with the maximum growth rate. Unlike the non-oscillatory case these equations

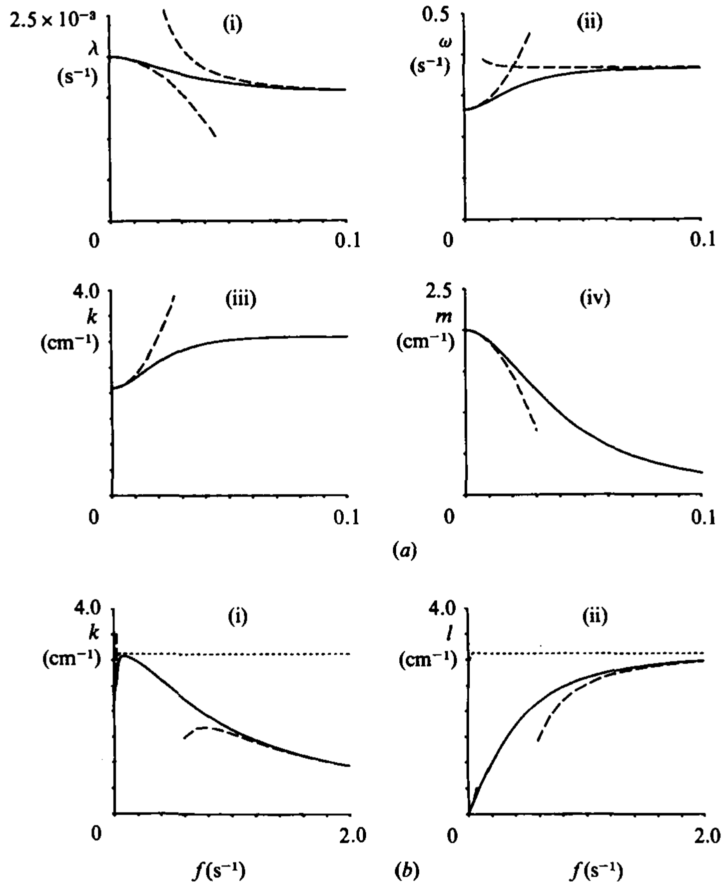


FIGURE 2. Graphs of the fastest-growing oscillatory instability for $\beta\bar{S}_x = 2.76\times10^{-5}\,\mathrm{cm}^{-1}$, $\alpha\bar{T}_z = -1.12\times10^{-3}\,\mathrm{cm}^{-1}$, and $\beta\bar{S}_z = -1.25\times10^{-3}\,\mathrm{cm}^{-1}$, with $\nu = 1.1\times10^{-2}\,\mathrm{cm}^2\,\mathrm{s}^{-1}$, $\kappa_T = 1.4\times10^{-3}\,\mathrm{cm}^2\,\mathrm{s}^{-1}$, and $\kappa_S = 1.1\times10^{-5}\,\mathrm{cm}^2\,\mathrm{s}^{-1}$. (*a*) shows (i) $\lambda$, (ii) $\omega$, (iii) $k$ and (iv) $m$ plotted against $f$ for values of $f$ up to $0.1\,\mathrm{s}^{-1}$. (*b*) shows (i) $k$ and (ii) $l$ for values of $f$ up to $2\,\mathrm{s}^{-1}$ with the dotted line showing $\mu$. The dashed lines are the asymptotics for small and large $f$.

do not yield a simple dependence of the fastest-growing mode on the rotation rate. Instead the behaviour of the oscillatory modes when rotation is added is investigated numerically. These investigations take the fastest-growing mode for a non-rotating system and see how this mode changes as the rotation rate is varied while keeping the temperature and salinity gradients fixed. Some results are shown in figures 2 and 3. These show how the growth rate $\lambda$, the components of the wave vector ($k$, $l$ and $m$), the wavenumber ($\mu$) and the frequency of the oscillation ($\omega$) change as the rotation rate is increased.

Initially, as $f$ is increased from zero, the instabilities develop an along-front slope with $l/k$ positive. When $f$ becomes of order $\nu\mu_0^2$ the fastest-growing mode undergoes a change of orientation so that its wavenumber vector becomes almost horizontal. Unlike the non-oscillatory case, this change is associated with changes in $\lambda$, $\mu$ and $k/m$. The wavenumber vector initially becomes almost perpendicular to the front as it becomes horizontal.

After this initial change $\lambda$, $\omega$ and $\mu$ remain virtually unaltered as $f$ is increased

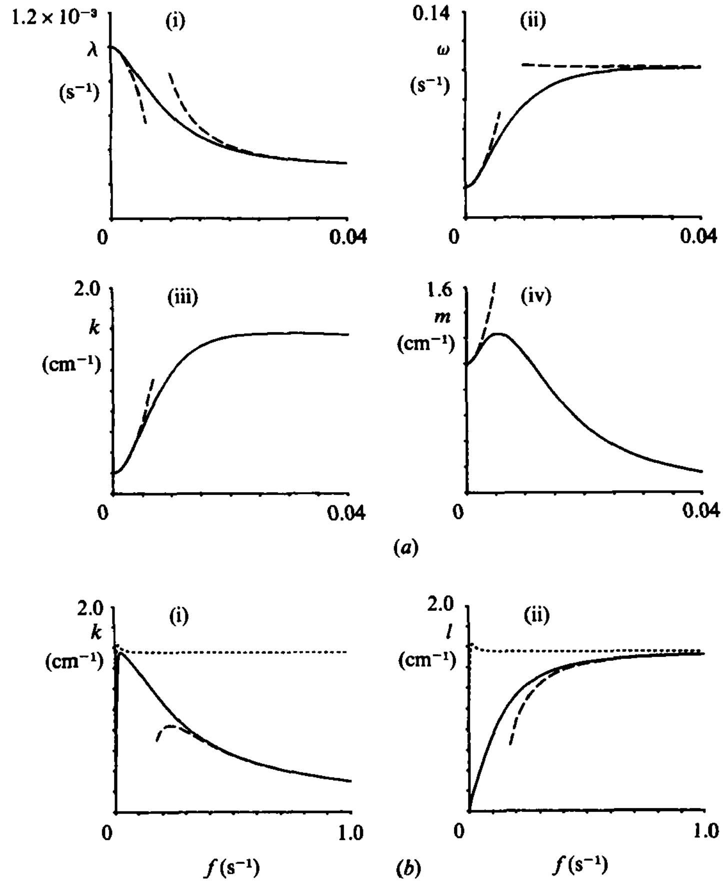


FIGURE 3. Graphs of the fastest-growing oscillatory instability for $\beta\bar{S}_x = 4.90\times10^{-6}\ \mathrm{cm^{-1}}$, $\alpha\bar{T}_z = -8.60\times10^{-5}\ \mathrm{cm^{-1}}$, and $\beta\bar{S}_z = -9.65\times10^{-5}\ \mathrm{cm^{-1}}$, with $\nu = 1.1\times10^{-2}\ \mathrm{cm^2\,s^{-1}}$. $\kappa_T = 1.4\times10^{-3}\ \mathrm{cm^2\,s^{-1}}$, and $\kappa_S = 1.1\times10^{-5}\ \mathrm{cm^2\,s^{-1}}$. (*a*) shows (i) $\lambda$, (ii) $\omega$, (iii) $k$ and (iv) $m$ plotted against $f$ for values of $f$ up to $0.04\ \mathrm{s^{-1}}$. (*b*) shows (i) $k$ and (ii) $l$ for values of $f$ up to $1\ \mathrm{s^{-1}}$ with the dotted line showing $\mu$. The dashed lines are the asymptotics for small and large $f$.

further. However, the wavenumber vector shifts its orientation from being almost perpendicular to the front to being parallel to it.

In order to check some of the properties of these graphs one can obtain asymptotic expansions for small and large $f$. These, which are superimposed on the graphs in figures 2 and 3, were obtained by substituting power-series expansions in $f$ into (4.3*a*) and (4.3*b*) and solving for each power of $f$. The expansions for small $f$ were of the form

$$(\lambda, k, m, \omega) = (\lambda_0, k_0, m_0, \omega_0) + f^2(\lambda_2, k_2, m_2, \omega_2) + \dots,$$

$$l = f l_1 + f^3 l_3 + \dots,$$

and for large $f$

$$(\lambda, l, \omega) = (\lambda_0, l_0, \omega_0) + f^{-2}(\lambda_2, l_2, \omega_2) + \dots,$$

$$(k, m) = f^{-1}(k_1, m_1) + f^{-3}(k_3, m_3) + \dots .$$

In all cases the asymptotics are for the first two terms only.

## 5. Conclusions

In this paper we investigate an unbounded stratified, rotating fluid with compensating gradients of heat and salt. We carry out a linear-stability analysis using molecular diffusivities, and find that the fluid can be unstable to either direct modes or oscillatory modes. We show that, provided there are horizontal heat and salt gradients, the fluid is always unstable to a non-oscillatory mode and that the fastest-growing mode has the same growth rate, wavenumber and across-front slope as the non-rotating case investigated by Holyer (1983). The wave vector becomes horizontal and aligns itself with the front as the rotation rate becomes of order $\nu\mu^2$. This changing of the orientation of the intrusions is such that the fluid does not have an along-front component to its velocity but moves in the direction of the horizontal temperature and salinity gradients.

The fastest-growing oscillatory instability is also found to change its orientation so that its wave vector becomes horizontal and aligns itself with the front. In this case, however, the two effects happen separately. Initially the wave vector becomes horizontal when the rotation rate is of order $\nu\mu^2$. This transition is accompanied by variations in $\lambda$, $k/m$, $\mu$ and $\omega$. As the rotation rate is increased further the fastest-growing mode aligns itself with the front. This second transition is associated with almost constant $\lambda$, $\mu$ and $\omega$.

Holyer (1983) found that for the non-rotating case the non-oscillatory disturbances grew faster than the oscillatory disturbances except when $\overline{T}_z$ is negative, $\beta\overline{S}_z/\alpha\overline{T}_z$ lies between 1 and $(\sigma+1)/(\sigma+\tau)$ and $\beta\overline{S}_x/\alpha\overline{T}_z$ is small. The non-oscillatory disturbances will also grow faster in the rotating case if the same conditions on the gradients hold. When these conditions are satisfied the oscillatory disturbance tends to have small $m$ and is relatively unaffected by the rotation.

Thus in the ocean environment you would not expect to observe the oscillatory interleaving, though it might be possible to see it in the laboratory.

The first author would like to thank the Science and Engineering Research Council for providing financial support.

### REFERENCES

BAINES, P. G. & GILL, A. E. 1969 On thermohaline convection with linear gradients. *J. Fluid Mech.* **37**, 289.

GREGG, M. C. 1980 The three-dimensional mapping of a small thermohaline intrusion. *J. Phys. Oceanogr.* **10**, 1468.

HOLYER, J. Y. 1983 Double-diffusive interleaving due to horizontal gradients. *J. Fluid Mech.* **137**, 347.

HORNE, E. P. W. 1978 Interleaving at the subsurface front in the slope water off Novia Scotia. *J. Geophys. Res.* **83**, 3659.

KNOBLOCH, E. & SPRUIT, H. C. 1983 The molecular weight barrier and angular momentum transport in radiative stellar interiors. *Astron. Astrophys.* **125**, 59.

MCDOUGALL, T. J. 1985 Double-diffusive interleaving I. *J. Phys. Oceanogr.* (in press).

POSMENTIER, E. S. & HIBBARD, C. B. 1982 The role of tilt in double diffusive interleaving. *J. Geophys. Res.* **87**, 518.

RUDDICK, B. R. & TURNER, J. S. 1979 The vertical length scale of double-diffusive intrusions. *Deep-Sea Res.* **26**, 903.

STERN, M. E. 1967 Lateral mixing of water masses. *Deep-Sea Res.* **14**, 747.

STOMMEL, H. & FEDOROV, K. N. 1967 Small scale structure in temperature and salinity near Timor and Mindanao. *Tellus* **19**, 306.

THORPE, S. A., HUTT, P. K. & SOULSBY, R. 1969 The effects of horizontal gradients on thermohaline convection. *J. Fluid Mech.* **38**, 375.

TOOLE, J. M. & GEORGI, D. T. 1981 On the dynamics and effects of double-diffusively driven intrusions. *Prog. Oceanogr.* **10**, 123.

WIRTZ, R. A., BRIGGS, D. G. & CHEN, C. F. 1972 Physical and numerical experiments on layered convection in a density-stratified fluid. *Geophys. Fluid Dyn.* **3**, 265.

WORTHEM, S., MOLLO-CHRISTENSEN, E. & OSTAPOFF, F. 1983 Effects of rotation and shear on doubly diffusive instability. *J. Fluid Mech.* **133**, 297.